

Identifying Majorana bound states at quantum spin Hall edges using a metallic probe

Bo Lu,¹ Guanxin Cheng,¹ Pablo Burset,² and Yukio Tanaka³

¹Center for Joint Quantum Studies and Department of Physics, Tianjin University, Tianjin 300072, China

²Department of Theoretical Condensed Matter Physics, Condensed Matter Physics Center (IFIMAC) and Instituto Nicolás Cabrera, Universidad Autónoma de Madrid, 28049 Madrid, Spain

³Department of Applied Physics, Nagoya University, Nagoya 464-8603, Japan

(Dated: April 12, 2022)

We study the conductance afforded by a normal-metal probe which is directly contacting the helical edge modes of a quantum spin Hall insulator (QSHI). We show a $2e^2/h$ conductance peak at zero temperature in QSHI-based superconductor-ferromagnet hybrids due to the formation of a single Majorana bound state (MBS). In a corresponding Josephson junction hosting a pair of MBSs, a $4e^2/h$ conductance peak is found at zero temperature. The conductance quantization is robust to changes of the relevant system parameters and, remarkably, remains unaltered with increasing the distance between probe and MBSs. In the low temperature limit, the conductance peak is robust as the probe is placed within the localization length of MBSs. Our findings can therefore provide an effective way to detect the existence of MBSs in QSHI systems.

I. INTRODUCTION

A quantum spin Hall insulator (QSHI) is a two dimensional (2D) topological insulator featuring topologically protected one dimensional (1D) edge states [1–7]. These edge states are termed *helical* since they circulate in reversed directions with opposite spin orientations. QSHIs have been realized using HgTe [8–11] and InAs/GaSb [12] quantum wells, among others [13–15], and are attracting significant attention as a platform for the creation and manipulation of Majorana bound states (MBSs); a very promising building-block for fault-tolerant quantum computations [16–24]. Signatures of MBSs include a fractional, or 4π -periodic, Josephson effect in QSHI-mediated junctions [25, 26], which has been recently observed [27–29]. Similar signatures of MBSs have been predicted in ferromagnetic-superconductor (FS) junctions proximity-induced at the helical edge of a QSHI, hosting a single MBS [26, 30], or a pair of them for SFS junctions [16, 25, 26].

Another basic transport signature of helical edge states is a quantized tunneling conductance in units of e^2/h , with e being the electron charge and h the Planck constant. Since the helical edge states of a QSHI comprise *one half* of a spin degenerate 1D electron gas, each edge can provide a quantized ballistic conductance of e^2/h over several micrometers [8, 31, 32]. When coupled to a superconductor, the conductance per edge is doubled ($2e^2/h$) [33] as a result of the perfect Andreev reflection of the helical states [34–36]. Consequently, a MBS in a QSHI is predicted to feature a quantized gate-voltage-averaged conductance peak [37]. Indeed, experimental evidence of MBSs in other topological systems has focused on measuring a robust quantization of zero-bias conductance peaks (ZBCPs) [38–51].

In this article, we propose to detect MBSs in the helical edge state via a normal probe terminal, such as an STM tip, coupled to the edge states (Fig. 1). We only

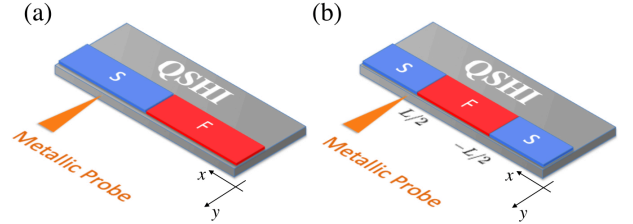


FIG. 1. Schematics of the three-terminal setup. FS (a) and SFS (b) junctions based on a single QSHI edge, with a biased one-dimensional normal-metal probe terminal.

consider one edge, assuming negligible overlap between different edge states due to a large width of the QSHI. A similar three-terminal setup with a metallic tip has been proposed to detect the helical nature of the edge states or to design novel applications [52–59]. Here, we focus on the detection of MBSs and consider both superconducting and magnetic regions, which open gaps on the helical edge channel forming the FS and SFS junctions featured in, respectively, Fig. 1(a) and Fig. 1(b). In the beam-splitter configuration, a bias voltage V at the probe terminal injects a current I into the helical edge state, propagating along it until is collected by distant grounded contacts. When the FS junction hosts a single MBS (or a pair for the SFS junction), the conductance dI/dV at the probe terminal reaches a quantized plateau of $2e^2/h$ ($4e^2/h$) at zero bias. The conductance quantization is robust under the change of all relevant system parameters. Strikingly, the quantization is also independent of the position of the probe terminal along the edge, which is in contrast to the decaying local density of states of MBSs. The ZBCP at finite temperature is suppressed due to thermal broadening but remains observable in the low temperature limit as the probe is placed within the localization length of MBSs. Such a zero-bias coherent transport effect thus provides an experimental signature

of MBSs in a QSHI.

II. MODEL AND FORMULAS

Model.— Our setup consists of a semi-infinite normal probe on the y axis and a QSHI edge lying along the x direction (Fig. 1). We set the origin at the FS boundary, or at the middle of the SFS, and place the contact point between the QSHI edge and the probe terminal at $(x_c, 0)$. The Hamiltonian is $\hat{H} = \frac{1}{2}\Psi^\dagger H \Psi$, with $H = H_N + H_T + H_j$, $\Psi = (\psi_\uparrow, \psi_\downarrow, \psi_\uparrow^\dagger, \psi_\downarrow^\dagger)^T$, and $\psi_{\uparrow(\downarrow)}$ the field operators for right (left) movers. H_N describes the normal probe terminal with a standard parabolic dispersion

$$H_N = \left(-\frac{\hbar^2 \partial_y^2}{2m_N} - \mu_N \right) \hat{\tau}_z \Theta(y) + U \hat{\tau}_z \delta(y - 0^+), \quad (1)$$

where m_N , μ_N , and $\hat{\tau}_{i=x,y,z}$ are the effective mass, chemical potential of normal probe, and Pauli matrices in the Nambu space. $\Theta(y)$ and $\delta(y)$ are the Heaviside and delta functions, respectively, and U is the barrier parameter between the probe and the QSHI. The bare helical edge states are described by the Hamiltonian

$$H_T = -i\hbar v_t \hat{\sigma}_z \partial_x - \mu_T \hat{\tau}_z, \quad (2)$$

where v_t is the Fermi velocity, μ_N is the chemical potential measured from the Dirac point of the helical states, and $\hat{\sigma}_{i=x,y,z}$ are Pauli matrices in the spin space. Finally, H_j describes the proximity-induced terms in the helical state with $j = 1$ ($j = 2$) corresponding to the FS (SFS) junction. Specifically,

$$H_1 = M_x \hat{\sigma}_x \hat{\tau}_z \Theta(-x) - \Delta \hat{\sigma}_y \hat{\tau}_y \Theta(x), \quad (3)$$

$$H_2 = M_x \hat{\sigma}_x \hat{\tau}_z \Theta\left(\frac{L}{2} - |x|\right) - \Delta \hat{\sigma}_y \hat{\tau}_y e^{i\chi_L} \Theta\left(-x - \frac{L}{2}\right) - \Delta \hat{\sigma}_y \hat{\tau}_y e^{i\chi_R} \Theta\left(x - \frac{L}{2}\right). \quad (4)$$

Here, M_x is an exchange field from the coupling to a ferromagnetic insulator and Δ is the proximity-induced pair potential from a conventional s -wave superconductor. For the SFS junction, L is the width of the F region and $\chi_{L,R}$ are the macroscopic superconducting phases, with $\chi = \chi_L - \chi_R$ being their difference.

The scattering wave function for the normal probe is

$$\Psi_{N\sigma} = \Phi_\sigma + b_{\uparrow\sigma} \hat{B}_\uparrow e^{iqy} + b_{\downarrow\sigma} \hat{B}_\downarrow e^{iqy} + a_{\uparrow\sigma} \hat{A}_\uparrow e^{-iqy} + a_{\downarrow\sigma} \hat{A}_\downarrow e^{-iqy}, \quad (5)$$

for an incident electron with spin $\sigma = \uparrow$ (\downarrow) and wave function $\Phi_\uparrow = (1, 0, 0, 0)^T e^{-iqy}$ [$\Phi_\downarrow = (0, 1, 0, 0)^T e^{-iqy}$]. Under the wide band approximation ($\mu_N \gg E$), the wave vector is $q = \sqrt{2m_N \mu_N} / \hbar$ and the spinors are $\hat{B}_\uparrow = (1, 0, 0, 0)^T$, $\hat{B}_\downarrow = (0, 1, 0, 0)^T$, $\hat{A}_\uparrow = (0, 0, 1, 0)^T$,

and $\hat{A}_\downarrow = (0, 0, 0, 1)^T$. The normal (Andreev) reflection amplitudes are $b_{\sigma'\sigma}$ ($a_{\sigma'\sigma}$) for an incoming electron of spin σ scattered as an electron (hole) of spin σ' .

At the edge of QSHI [60–65], the solutions on the F region are $\hat{F}_1 = N_1^{-1}(\hbar v_t \kappa_e + \mu_T, M_x, 0, 0)^T e^{i\kappa_e x}$, $\hat{F}_2 = N_2^{-1}(M_x, \hbar v_t \kappa_e + \mu_T, 0, 0)^T e^{-i\kappa_e x}$, $\hat{F}_3 = N_3^{-1}(0, 0, \hbar v_t \kappa_h + \mu_T, M_x)^T e^{-i\kappa_h x}$, and $\hat{F}_4 = N_4^{-1}(0, 0, M_x, \hbar v_t \kappa_h + \mu_T)^T e^{i\kappa_h x}$, with wave vectors $\kappa_{e(h)} = \sqrt{\mu_T^2 - M_x^2} / \hbar v_t$ for $M_x < \mu_T$, and $\kappa_{e(h)} = \pm i \sqrt{M_x^2 - \mu_T^2} / \hbar v_t$ for $M_x > \mu_T$. $N_{i=1\sim 4}$ are normalization factors. On the S region we find $\hat{S}_1 = (u, 0, 0, v)^T e^{ik^+ x}$, $\hat{S}_2 = (0, -u, v, 0)^T e^{-ik^+ x}$, $\hat{S}_3 = (0, -v, u, 0)^T e^{-ik^- x}$, and $\hat{S}_4 = (v, 0, 0, u)^T e^{ik^- x}$, with $u(v) = \sqrt{(E \pm \sqrt{E^2 - \Delta^2}) / 2E}$, wave vector $k^\pm = k_T \pm \sqrt{E^2 - \Delta^2} / (\hbar v_t)$ and $k_T = \mu_T / (\hbar v_t)$. An incident spin- σ electron from the normal probe thus has a transmitted wave function $\Psi_{T\sigma}(x)$ on the QSHI side, which is a suitable superposition of spinors $\hat{F}_{i=1\sim 4}$ and $\hat{S}_{i=1\sim 4}$.

To determine the scattering amplitudes, we match $\Psi_{N\sigma}$ and $\Psi_{T\sigma}$ at the contact using the boundary conditions [59, 66, 67]

$$\Psi_{N\sigma}(y = 0^+) = c \Psi_{T\sigma}(x_c^-) + c \Psi_{T\sigma}(x_c^+), \quad (6)$$

$$\hat{K} \Psi_{N\sigma}(y = 0^+) = i v_t [\Psi_{T\sigma}(x_c^-) - \Psi_{T\sigma}(x_c^+)], \quad (7)$$

with $\hat{K} = \hbar c \hat{\sigma}_z \hat{\tau}_z (m_N^{-1} \partial_y - 2U / \hbar^2)$. The parameter $Z = m_N U / (\hbar^2 q)$ describes the barrier strength between the probe and the helical edge, while the real and dimensionless number c represents the different microscopic details between them, such as the hopping integrals in the underlying lattice model [59, 66, 67].

When a bias voltage V is applied to the normal probe, the conductance G at zero temperature is calculated using the formula [68]

$$G = \frac{e^2}{h} \sum_{\sigma\sigma'} \left(\delta_{\sigma\sigma'} + |a_{\sigma\sigma'}|^2 - |b_{\sigma\sigma'}|^2 \right). \quad (8)$$

Here, $a_{\sigma\sigma'}$ and $b_{\sigma\sigma'}$ are reflection amplitudes at $E = eV$.

For the numerical calculations we choose $v_N \approx 1.57 \times 10^6$ m/s and $\mu_N \approx 7.0$ eV, corresponding to copper; $v_t \approx 5.5 \times 10^5$ m/s and $\mu_T \approx 0.01$ eV for HgCdTe quantum wells; and $\Delta \approx 0.1$ meV, which corresponds to a proximity-induced gap from a niobium superconductor. For simplicity, we only consider the short junction for the SFS geometry, with $k_T L \ll \mu_T / \Delta$, and choose $k_T L = 2$ so that the width of F is $L \approx 70$ nm. We note that our main conclusions are not material dependent.

III. FS JUNCTION

We start with the FS junction [Fig. 1(a)] and analyze the conductance probed by a normal-metal terminal posi-

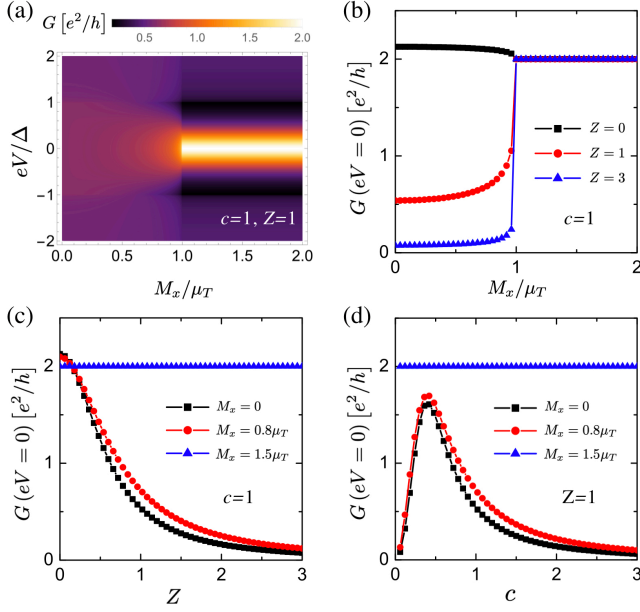


FIG. 2. Zero-temperature conductance on the normal-metal terminal placed at the FS boundary. (a) The conductance spectra at zero temperature as a function of the energy eV and magnetization M_x for $c = 1$ and $Z = 1$. (b), (c), and (d) show the zero-bias conductance as a function of M_x , Z , and c , respectively. We set $c = 1$ for (b) and (c), and $Z = 1$ for (d).

tioned at the boundary between the magnetic and superconducting regions, where the MBS is spatially localized. For $M_x < \mu_T$, the magnetic gap is buried beneath the Fermi level and there are propagating channels in the F region, whereas a magnetic gap starts to develop near the Fermi surface when $M_x > \mu_T$. The critical point between these two topological phases is thus $M_x = \mu_T$. This phase boundary clearly appears in the conductance dependence on the magnetization M_x , see Fig. 2(a). The conductance for $M_x > \mu_T$ clearly showcases the celebrated Majorana zero-bias peak with quantized height $2e^2/h$ [69–79], and also features a dip at the gap edge. Reducing M_x from μ_T towards 0, the value of the ZBCP loses its quantization and can either increase when Z is small or decrease for large Z , see Fig. 2(b). Figure 2(c) and Fig. 2(d) show that the quantized value of the ZBCP is immune to variations of the parameters Z and c , respectively, when in the topological phase with $M_x > \mu_T$. The robust $2e^2/h$ value indicates the presence of a single MBS. However, in the trivial phase ($M_x < \mu_T$) the conductance dependence on c and Z is very different. First, for $Z = 0$ the metallic probe is transparently coupled to the helical state and all the injected current at zero bias can either directly flow to the drain in F or undergo a perfect Andreev reflection on S. This results in a conductance value slightly bigger than $2e^2/h$, which can not be achieved in the absence of a tip when the bias is applied to the F region. For $Z \neq 0$, electrons incoming

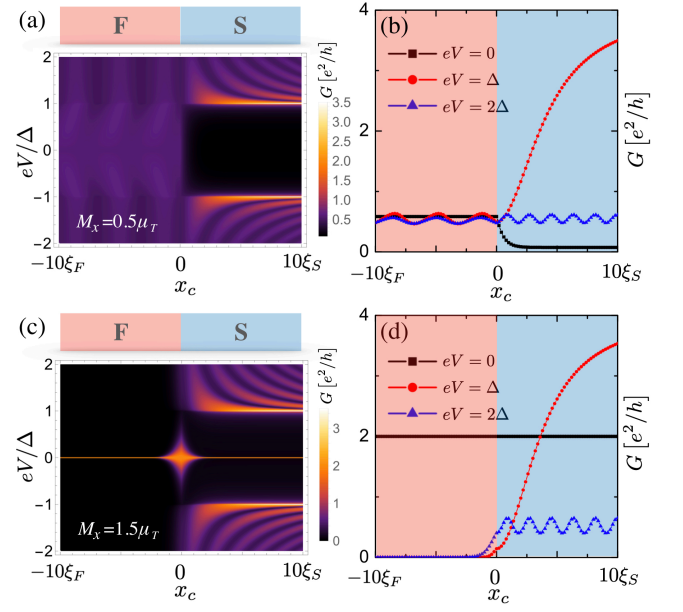


FIG. 3. Spatial dependence of the probe conductance at zero temperature for the FS junction. (a,b) In the trivial phase with $M_x/\mu_T = 0.5$, (a) conductance spectra as a function of the bias eV and the position x_c , and (b) three cuts corresponding to biases $eV = 0, \Delta$ and 2Δ . (c,d) Same as before for the topological phase with $M_x/\mu_T = 1.5$. The scale of the horizontal axis is different in each region since $\xi_F \ll \xi_S$. In all cases, $c = 1$ and $Z = 1$.

from the tip can backscatter, thus monotonically reducing the conductance as Z increases. By contrast, the dependence on c of the ZBCP displays a non-monotonic behavior in the trivial phase. The conductance is suppressed for $c \rightarrow 0, \infty$, since the probe is decoupled from the edge state in these limits, and thus exhibits a maximum in between, whose position depends on both c and Z [59].

When the probe is at the FS boundary, we have shown a perfectly quantized ZBCP in the topological phase $M_x > \mu_T$. However, this exact position may be challenging to reach in experiments, so we now consider the spatial dependence of the conductance as the probe moves along the QSHI edge. First, it is convenient to define two characteristic length scales: $\xi_F = \hbar v_t/\mu_T$ inside F and $\xi_S = \hbar v_t/\Delta$ in S. Figure 3 shows the dependence on the coordinate x of the conductance at the normal terminal probe. As expected, there is no quantized ZBCP in the trivial phase ($M_x < \mu_T$), see Fig. 3(a) and Fig. 3(b). In this regime, the tip conductance in the F region features small oscillations around a constant value, while it displays a gapped profile with large peaks at $|eV| = \Delta$ in the S region, induced by the density of states in a uniform superconductor.

By contrast, the topological phase ($M_x > \mu_T$) shown in Fig. 3(c) and Fig. 3(d) presents a remarkable result. The zero bias conductance is not only quantized at the

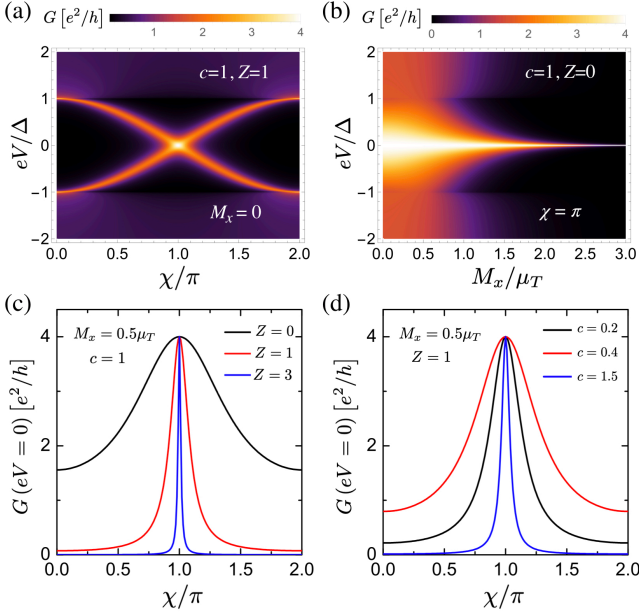


FIG. 4. Zero-temperature conductance of a normal-metal probe placed in the middle of an SFS junction. (a) Conductance versus applied voltage and phase difference χ for $M_x = 0$ and $Z = c = 1$. (b) For fixed $\chi = \pi$, conductance versus eV and M_x , with $Z = 0$ and $c = 1$. (c,d) Zero bias conductance as a function of χ for $M_x = 0.5\mu_T$ and several values of Z (c) or c (d). We set $c = 1$ for (c) and $Z = 1$ for (d).

FS boundary, but also maintains a constant value of $2e^2/h$ for *every position* along the QSHI edge. The emergence of such a robust ZBCP seems exotic, especially for $x_c \rightarrow +\infty$, i.e., several coherence lengths (ξ_S) away from the localized MBS. We note that the *bulk* proximitized superconducting region ($x_c \rightarrow +\infty$) is fully gapped at zero energy, without free quasiparticles and with the local density of the MBS greatly suppressed [60, 61, 63, 65, 78]. To further analyze this counter-intuitive result, we examine the zero-bias scattering amplitudes for $x_c > 0$ in the topological phase with $M_x > \mu_T$, namely,

$$b_{\uparrow\uparrow} = -[c^4(i + 2Z)^2 + \eta^2] \Xi^{-1}, \quad (9a)$$

$$a_{\uparrow\uparrow} = -e^{-2ik_T x_c} \Omega_+ [c^4 + (2c^2 Z - i\eta)^2] \Xi^{-1}, \quad (9b)$$

$$b_{\uparrow\downarrow(\downarrow\uparrow)} = \pm i e^{\pm 2ik_T x_c} \Omega_{\mp} [c^2(i + 2Z) \pm i\eta]^2 \Xi^{-1}, \quad (9c)$$

$$a_{\uparrow\downarrow(\downarrow\uparrow)} = -i [c^4(1 + 4Z^2) \mp 2c^2\eta + \eta^2] \Xi^{-1}, \quad (9d)$$

with $\Omega_{\pm} = M_x/(\pm i\mu_T + \sqrt{M_x^2 - \mu_T^2})$, $\Xi = 2[c^4(1 + 4Z^2) + \eta^2]$, $\eta = v_t/v_N$, $a_{\downarrow\downarrow} = -a_{\uparrow\uparrow}^*$ and $b_{\downarrow\downarrow} = b_{\uparrow\uparrow}$. The spacial dependence at zero energy appears as global phase factors $e^{\pm 2ik_T x_c}$, so the resulting conductance is thus quantized and independent of the position x_c . This effect provides an interesting signature of the existence of MBS in a QSHI.

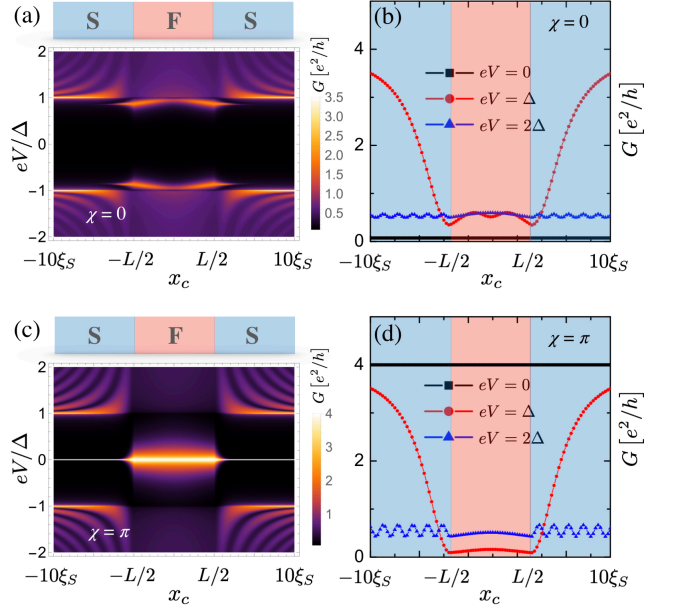


FIG. 5. Spatial dependence of the probe conductance at zero temperature for an SFS junction. (a, b) For $\chi = 0$, (a) conductance spectra as a function of bias and position, and (b) three cuts corresponding to biases $eV = 0, \Delta$ and 2Δ . (c,d) Same as before for $\chi = \pi$. In all cases, we set $M_x = 0.5\mu_T$, $Z = 1$, and $c = 1$.

IV. SFS JUNCTION

We now connect the normal-metal terminal probe to the SFS junction. First, we place it in the middle of F and study the conductance as a function of M_x and the superconducting phase difference χ in Fig. 4. At zero magnetization [Fig. 4(a)], a resonance peak inside the superconducting gap indicates the presence of a pair of MBSs exhibiting a protected crossing at $\chi = \pi$. The robustness of the crossing point is shown in Fig. 4(b), where the zero biased conductance is quantized with $G = 4e^2/h$ for $\chi = \pi$ and arbitrary M_x , similar to works in other topological Josephson junctions [80–82]. Indeed, the QSHI-mediated Josephson junction is in the topological phase independently of the magnetization [26, 72]. For nonzero eV , the transition between a dominant superconducting gap into a dominant magnetic one can be seen around $M_x = \mu_T$; as the magnetic gap becomes dominant for $M_x > \mu_T$, the conductance is suppressed. Figure 4(c) and Fig. 4(d) show the robustness of the ZBCP at $\chi = \pi$ against the coupling parameters c and Z .

Next, we compare the spacial dependence of the probe conductance for $\chi = 0$ [Fig. 5(a) and Fig. 5(b)] and $\chi = \pi$ [Fig. 5(c) and Fig. 5(d)]. For $\chi = 0$, there is no ZBCP in the SFS junction since the MBSs have merged with the continuum. By contrast, at the crossing $\chi = \pi$, the zero-bias conductance becomes perfectly quantized to $4e^2/h$. As it was the case for the FS junction in the topological

phase, the normal probe conductance remains quantized for any position across the whole SFS junction. However, the quantized ZBCP is now present for any value of M_x , and is broadened in the F region, cf. Fig. 4(c). Analytically, when the probe is on the left S side ($x_c < -L/2$), the coefficients are obtained as

$$b_{\uparrow\uparrow(\downarrow\downarrow)} = -(1 + e^{i\chi}) \Upsilon_1 / (\Upsilon_2 \pm \Upsilon_3), \quad (10a)$$

$$a_{\downarrow\uparrow(\uparrow\downarrow)} = \mp \Upsilon_4 / (\Upsilon_2 \pm \Upsilon_3), \quad (10b)$$

and $b_{\uparrow\downarrow} = b_{\downarrow\uparrow} = a_{\uparrow\uparrow} = a_{\downarrow\downarrow} = 0$, with $\Upsilon_1 = c^4(i + 2Z)^2 + \eta^2$, $\Upsilon_2 = (1 + e^{i\chi})(c^4 + 4c^4Z^2 + \eta^2)$, $\Upsilon_3 = 2c^2(e^{i\chi} - 1)\eta e^{\Delta(L+2x_c)/(\hbar v_i)}$ and $\Upsilon_4 = 2ic^2(1 + e^{i\chi})\eta - i\Upsilon_3$. As the phase bias is $\chi = \pi$, $b_{\sigma\sigma}$ becomes 0 while $a_{\uparrow\uparrow} = a_{\downarrow\downarrow} = i$ exhibiting perfect Andreev reflection, regardless of the position of probe.

V. TEMPERATURE EFFECT

So far we have reported that the ZBCP always sticks to the quantized value at zero temperature. To obtain a result that can be directly compared to experiments, we next remark on the temperature effect. At zero temperature, we find that the topological ZBCP becomes sharper as the probe is placed far from the localized MBSs, see Fig. 3(c) and Fig. 5(c). This indicates that the height of the ZBCP would be lowered at finite temperatures due to the thermal broadening. We calculate the conductance at finite temperature T as

$$g(V) = \int_{-\infty}^{+\infty} d\varepsilon G(\varepsilon) \left[4k_B T \cosh^2 \left(\frac{\varepsilon - eV}{2k_B T} \right) \right]^{-1}, \quad (11)$$

where $G(\varepsilon)$ is the conductance at zero temperature given in Eq. (8). We find that the ZBCP height does not change significantly by increasing the temperature T as the probe tip is placed at $x_c = 0$, i.e., the interface of the FS junction or the middle of the SFS junction, as shown in Fig. 6. However, a finite temperature has a drastic suppression effect on the ZBCP height as the tip moves far away from $x_c = 0$. This is consistent with recent experiments where a robust ZBCP was found around the FS interface at finite temperature [83]. Our results show that the weakened ZBCP is still observable if the probe is within the localization length of the MBSs at low temperature, e.g., $x_c = 0.1\xi_S$ (red line in Fig. 6(b)) in the SFS junction. Consequently, the unusual spatial independence of the ZBCP found in our calculation could be experimentally observed in low temperature measurements.

VI. CONCLUSION

We studied the conductance afforded by a normal-metal probe which directly contacts the helical edge

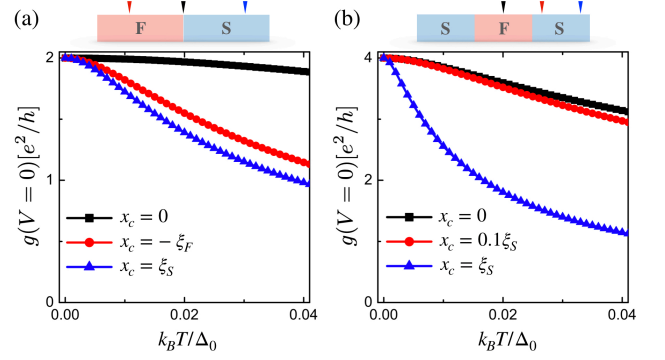


FIG. 6. Zero-biased conductance as a function of temperature T for different positions of the probe. (a) The probe is placed at $x_c = 0, -\xi_F$, and ξ_S in the FS junction. The parameters of the FS junction are the same as Fig. 3(c). (b) The probe is placed at $x_c = 0, 0.1\xi_S$, and ξ_S in the SFS junction with the same parameters as in Fig. 5(c). Δ_0 is the superconducting gap at zero temperature.

modes of a quantum spin Hall insulator. We found a robust quantized zero-biased conductance peak in both FS and SFS junctions indicating the presence of Majorana bound states at each FS boundary. The conductance quantization is robust under variations of the parameters controlling the coupling between the tip and the helical edge state. Moreover, we found that the zero bias conductance quantization remains unchanged as we moved the probe along the edge, remarkably, even for distances much larger than the localization length of the Majorana states. This result can not be simply explained by the local density of states in the tunneling model [56–58]. Our analytical results suggested that the spatial independence of the zero-bias tip conductance results from a coherent coupling to the zero-energy MBSs. Finally, we discuss the temperature effect on the ZBCP to estimate the quality of the conductance quantization in actual experiments. Our proposal for the observation of Majorana states using a metallic probe is within reach of recent experimental advances implementing hybrid superconductor and magnetic structures on the quantum spin Hall insulator [15, 28, 29, 33, 83–87].

ACKNOWLEDGMENTS

B. L. acknowledges support from the National Natural Science Foundation of China (project 11904257) and the Natural Science Foundation of Tianjin (project 20JCQNJC01310). P. B. acknowledges support from the Spanish CM “Talento Program” Project no. 2019-T1/IND-14088 and the Spanish Ministerio de Ciencia e Innovación Grant no. PID2020-117992GA-I00. Y. T. was supported by Grant-in-Aid for Scientific Research on Innovative Areas and Grant-in-Aid for Scientific Re-

search B (Grant No. JP18H01176) from the Ministry of Education, Culture, Sports, Science, and Technology, Japan (MEXT). Y. T. was also supported by Grant-in-Aid for Scientific Research A (KAKENHI Grant No. JP20H00131) and the JSPS Core-to-Core program Oxide Superspin International Network.

-
- [1] C. L. Kane and E. J. Mele, “Quantum spin hall effect in graphene,” *Phys. Rev. Lett.* **95**, 226801 (2005).
 - [2] C. L. Kane and E. J. Mele, “ Z_2 topological order and the quantum spin hall effect,” *Phys. Rev. Lett.* **95**, 146802 (2005).
 - [3] B. A. Bernevig, T. L. Hughes, and S. C. Zhang, “Quantum spin Hall effect and topological phase transition in HgTe quantum wells,” *Science* **314**, 1757 (2006).
 - [4] Chaoxing Liu, Taylor L. Hughes, Xiao-Liang Qi, Kang Wang, and Shou-Cheng Zhang, “Quantum spin Hall effect in inverted type-II semiconductors,” *Phys. Rev. Lett.* **100**, 236601 (2008).
 - [5] Congjun Wu, B Andrei Bernevig, and Shou-cheng Zhang, “Helical Liquid and the Edge of Quantum Spin Hall Systems,” *Phys. Rev. Lett.* **96**, 106401 (2006).
 - [6] Cenke Xu and J. E. Moore, “Stability of the quantum spin Hall effect: Effects of interactions, disorder, and Z_2 topology,” *Phys. Rev. B* **73**, 045322 (2006).
 - [7] Chen-Hsuan Hsu, Peter Stano, Jelena Klinovaja, and Daniel Loss, “Helical liquids in semiconductors,” *Semiconductor Science and Technology* **36**, 123003 (2021).
 - [8] Markus König, Steffen Wiedmann, Christoph Brüne, Andreas Roth, Hartmut Buhmann, Laurens W. Molenkamp, Xiao-Liang Qi, and Shou-Cheng Zhang, “Quantum Spin Hall Insulator State in HgTe Quantum Wells,” *Science* **318**, 766–770 (2007).
 - [9] Markus König, Hartmut Buhmann, Laurens W. Molenkamp, Taylor Hughes, Chao-Xing Liu, Xiao-Liang Qi, and Shou-Cheng Zhang, “The quantum spin hall effect: Theory and experiment,” *Journal of the Physical Society of Japan* **77**, 031007 (2008).
 - [10] Andreas Roth, Christoph Brüne, Hartmut Buhmann, Laurens W. Molenkamp, Joseph Maciejko, Xiao-Liang Qi, and Shou-Cheng Zhang, “Nonlocal Transport in the Quantum Spin Hall State,” *Science* **325**, 294–297 (2010).
 - [11] Christoph Brüne, Andreas Roth, Hartmut Buhmann, Ewelina M. Hankiewicz, Laurens W. Molenkamp, Joseph Maciejko, Xiao-Liang Qi, and Shou-Cheng Zhang, “Spin polarization of the quantum spin Hall edge states,” *Nat. Phys.* **8**, 485–490 (2012).
 - [12] Ivan Knez, Rui-Rui Du, and Gerard Sullivan, “Evidence for Helical Edge Modes in Inverted InAs/GaSb Quantum Wells,” *Phys. Rev. Lett.* **107**, 136603 (2011).
 - [13] F. Reis, G. Li, L. Dudy, M. Bauernfeind, S. Glass, W. Hanke, R. Thomale, J. Schäfer, and R. Claessen, “Bismuthene on a SiC substrate: A candidate for a high-temperature quantum spin Hall material,” *Science* **357**, 287–290 (2017).
 - [14] J. Kammhuber, M. C. Cassidy, F. Pei, M. P. Nowak, A. Vuik, Ö. Gül, D. Car, S. R. Plissard, E. P. A. M. Bakkers, M. Wimmer, and L. P. Kouwenhoven, “Conductance through a helical state in an Indium antimonide nanowire,” *Nat. Commun.* **8**, 478 (2017).
 - [15] Sanfeng Wu, Valla Fatemi, Quinn D Gibson, Kenji Watanabe, Takashi Taniguchi, Robert J Cava, and Pablo Jarillo-Herrero, “Observation of the quantum spin Hall effect up to 100 Kelvin in a monolayer crystal,” *Science* **359**, 76–79 (2018).
 - [16] A Kitaev, “Unpaired majorana fermions in quantum wires,” *Physics-Uspekhi* **44**, 131–136 (2001).
 - [17] A. Kitaev, “Fault-tolerant quantum computation by anyons,” *Annals of Physics* **303**, 2 (2003).
 - [18] Chetan Nayak, Steven H. Simon, Ady Stern, Michael Freedman, and Sankar Das Sarma, “Non-abelian anyons and topological quantum computation,” *Rev. Mod. Phys.* **80**, 1083–1159 (2008).
 - [19] M. Z. Hasan and C. L. Kane, “Colloquium: Topological insulators,” *Rev. Mod. Phys.* **82**, 3045–3067 (2010).
 - [20] Xiao-Liang Qi and Shou-Cheng Zhang, “Topological insulators and superconductors,” *Rev. Mod. Phys.* **83**, 1057–1110 (2011).
 - [21] Jason Alicea, Yuval Oreg, Gil Refael, Felix von Oppen, and Matthew P. A. Fisher, “Non-abelian statistics and topological quantum information processing in 1d wire networks,” *Nature Physics* **7**, 412–417 (2011).
 - [22] Martin Leijnse and Karsten Flensberg, “Introduction to topological superconductivity and majorana fermions,” *Semiconductor Science and Technology* **27**, 124003 (2012).
 - [23] Yoichi Ando, “Topological insulator materials,” *Journal of the Physical Society of Japan* **82**, 102001 (2013).
 - [24] G. Tkachov and E. M. Hankiewicz, “Spin-helical transport in normal and superconducting topological insulators,” *physica status solidi (b)* **250**, 215–232 (2013).
 - [25] H.-J. Kwon, K. Sengupta, and V. M. Yakovenko, “Fractional ac josephson effect in p- and d-wave superconductors,” *The European Physical Journal B - Condensed Matter and Complex Systems* **37**, 349–361 (2004).
 - [26] Liang Fu and C. L. Kane, “Josephson current and noise at a superconductor/quantum-spin-Hall-insulator/superconductor junction,” *Phys. Rev. B* **79**, 161408 (2009).
 - [27] J. Wiedenmann, E. Bocquillon, R. S. Deacon, S. Hartinger, O. Herrmann, T. M. Klapwijk, L. Maier, C. Ames, C. Brüne, C. Gould, A. Oiwa, K. Ishibashi, S. Tarucha, H. Buhmann, and L. W. Molenkamp, “ 4π -periodic Josephson supercurrent in HgTe-based topological Josephson junctions,” *Nature Communications* **7**, 10303 (2016).
 - [28] Erwann Bocquillon, Russell S. Deacon, Jonas Wiedenmann, Philipp Leubner, Teunis M. Klapwijk, Christoph Brüne, Koji Ishibashi, Hartmut Buhmann, and Laurens W. Molenkamp, “Gapless Andreev bound states in the quantum spin Hall insulator HgTe,” *Nature Nanotechnology* **12**, 137–143 (2017).
 - [29] R. S. Deacon, J. Wiedenmann, E. Bocquillon, F. Domínguez, T. M. Klapwijk, P. Leubner, C. Brüne, E. M. Hankiewicz, S. Tarucha, K. Ishibashi, H. Buhmann, and L. W. Molenkamp, “Josephson radiation from gapless andreev bound states in hgte-based topological junctions,” *Phys. Rev. X* **7**, 021011 (2017).
 - [30] Liang Fu and C. L. Kane, “Superconducting proximity effect and Majorana fermions at the surface of a topological insulator,” *Phys. Rev. Lett.* **100**, 096407 (2008).
 - [31] C. Brüne, A. Roth, E. G. Novik, M. König, H. Buhmann, E. M. Hankiewicz, W. Hanke, J. Sinova, and

- L. W. Molenkamp, “Evidence for the ballistic intrinsic spin Hall effect in HgTe nanostructures,” *Nat. Phys.* **6**, 448–454 (2010).
- [32] Lingjie Du, Ivan Knez, Gerard Sullivan, and Rui-Rui Du, “Robust helical edge transport in gated InAs/GaSb bilayers,” *Phys. Rev. Lett.* **114**, 096802 (2015).
- [33] Ivan Knez, Rui-Rui Du, and Gerard Sullivan, “Andreev reflection of helical edge modes in InAs/GaSb quantum spin Hall insulator,” *Phys. Rev. Lett.* **109**, 186603 (2012).
- [34] P. Adroguer, C. Grenier, D. Carpentier, J. Cayssol, P. Degiovanni, and E. Orignac, “Probing the helical edge states of a topological insulator by Cooper-pair injection,” *Phys. Rev. B* **82**, 081303 (2010).
- [35] Qing-Feng Sun, Yu-Xian Li, Wen Long, and Jian Wang, “Quantum Andreev effect in two-dimensional HgTe/CdTe quantum well/superconductor systems,” *Phys. Rev. B* **83**, 115315 (2011).
- [36] Awadhesh Narayan and Stefano Sanvito, “Andreev reflection in two-dimensional topological insulators with either conserved or broken time-reversal symmetry,” *Phys. Rev. B* **86**, 041104 (2012).
- [37] Shuo Mi, D. I. Pikulin, M. Wimmer, and C. W. J. Beenakker, “Proposal for the detection and braiding of Majorana fermions in a quantum spin Hall insulator,” *Phys. Rev. B* **87**, 241405 (2013).
- [38] V. Mourik, K. Zuo, S. M. Frolov, S. R. Plissard, E. P. A. M. Bakkers, and L. P. Kouwenhoven, “Signatures of Majorana fermions in hybrid superconductor-semiconductor nanowire devices,” *Science* **336**, 1003 (2012).
- [39] M. T. Deng, C. L. Yu, G. Y. Huang, M. Larsson, P. Caroff, and H. Q. Xu, “Anomalous zero-bias conductance peak in a Nb-InSb nanowire-Nb hybrid device,” *Nano letters* **12**, 6414 (2012).
- [40] Eduardo J. H. Lee, Xiaocheng Jiang, Ramón Aguado, Georgios Katsaros, Charles M. Lieber, and Silvano De Franceschi, “Zero-bias anomaly in a nanowire quantum dot coupled to superconductors,” *Phys. Rev. Lett.* **109**, 186802 (2012).
- [41] Anindya Das, Yuval Ronen, Yonatan Most, Yuval Oreg, Moty Heiblum, and Hadas Shtrikman, “Zero-bias peaks and splitting in an Al-InAs nanowire topological superconductor as a signature of Majorana fermions,” *Nature Physics* **8**, 887–895 (2012).
- [42] M. T. Deng, S. Vaitiekunas, E. B. Hansen, J. Danon, M. Leijnse, K. Flensberg, J. Nygård, P. Krogstrup, and C. M. Marcus, “Majorana bound state in a coupled quantum-dot hybrid-nanowire system,” *Science* **354**, 1557 (2016).
- [43] Denis Chevallier and Jelena Klinovaja, “Tomography of Majorana fermions with STM tips,” *Phys. Rev. B* **94**, 035417 (2016).
- [44] S. M. Albrecht, A. P. Higginbotham, M. Madsen, F. Kuemmeth, T. S. Jespersen, J. Nygård, P. Krogstrup, and C. M. Marcus, “Exponential protection of zero modes in Majorana islands,” *Nature* **531**, 206–209 (2016).
- [45] Fabrizio Nichele, Asbjørn C. C. Drachmann, Alexander M. Whiticar, Eoin C. T. O’Farrell, Henri J. Suominen, Antonio Fornieri, Tian Wang, Geoffrey C. Gardner, Candice Thomas, Anthony T. Hatke, Peter Krogstrup, Michael J. Manfra, Karsten Flensberg, and Charles M. Marcus, “Scaling of Majorana zero-bias conductance peaks,” *Phys. Rev. Lett.* **119**, 136803 (2017).
- [46] Önder Gül, Hao Zhang, Jouri D. S. Bommer, Michiel W. A. de Moor, Diana Car, Sébastien R. Plissard, Erik P. A. M. Bakkers, Attila Geresdi, Kenji Watanabe, Takashi Taniguchi, and Leo P. Kouwenhoven, “Ballistic majorana nanowire devices,” *Nature Nanotechnology* **13**, 192–197 (2018).
- [47] Y. Tanaka and S. Kashiwaya, “Anomalous charge transport in triplet superconductor junctions,” *Phys. Rev. B* **70**, 012507 (2004).
- [48] Y. Tanaka, S. Kashiwaya, and T. Yokoyama, “Theory of enhanced proximity effect by midgap Andreev resonant state in diffusive normal-metal/triplet superconductor junctions,” *Phys. Rev. B* **71**, 094513 (2005).
- [49] Yukio Tanaka, Masatoshi Sato, and Naoto Nagaosa, “Symmetry and topology in superconductors –odd-frequency pairing and edge states–,” *Journal of the Physical Society of Japan* **81**, 011013 (2012).
- [50] Jorge Cayao and Pablo Buset, “Confinement-induced zero-bias peaks in conventional superconductor hybrids,” *Phys. Rev. B* **104**, 134507 (2021).
- [51] Shao-Pin Chiu, C. C. Tsuei, Sheng-Shiuan Yeh, Fu-Chun Zhang, Stefan Kirchner, and Juhn-Jong Lin, “Observation of triplet superconductivity in CoSi₂/TiSi₂ heterostructures,” *Science Advances* **7**, eabg6569 (2021).
- [52] V. Shivamoggi, G. Refael, and J. E. Moore, “Majorana fermion chain at the quantum spin hall edge,” *Phys. Rev. B* **82**, 041405 (2010).
- [53] Colin Benjamin and Jiannis K. Pachos, “Detecting majorana bound states,” *Phys. Rev. B* **81**, 085101 (2010).
- [54] Sourin Das and Sumathi Rao, “Spin-polarized scanning-tunneling probe for helical luttinger liquids,” *Phys. Rev. Lett.* **106**, 236403 (2011).
- [55] Björn Sothmann, Francesco Giazotto, and Ewelina M Hankiewicz, “High-efficiency thermal switch based on topological josephson junctions,” *New Journal of Physics* **19**, 023056 (2017).
- [56] Lennart Bours, Björn Sothmann, Matteo Carrega, Elia Strambini, Ewelina M. Hankiewicz, Laurens W. Molenkamp, and Francesco Giazotto, “Topological squipt based on helical edge states in proximity to superconductors,” *Phys. Rev. Applied* **10**, 014027 (2018).
- [57] Lennart Bours, Björn Sothmann, Matteo Carrega, Elia Strambini, Alessandro Braggio, Ewelina M. Hankiewicz, Laurens W. Molenkamp, and Francesco Giazotto, “Phase-tunable thermal rectification in the topological squipt,” *Phys. Rev. Applied* **11**, 044073 (2019).
- [58] Gianmichele Blasi, Fabio Taddei, Liliana Arrachea, Matteo Carrega, and Alessandro Braggio, “Nonlocal thermoelectricity in a superconductor–topological-insulator–superconductor junction in contact with a normal-metal probe: Evidence for helical edge states,” *Phys. Rev. Lett.* **124**, 227701 (2020).
- [59] Abhiram Soori, “Scattering in quantum wires and junctions of quantum wires with edge states of quantum spin hall insulators,” (2020), [arXiv:2005.11557 \[cond-mat.mes-hall\]](https://arxiv.org/abs/2005.11557).
- [60] François Crépin, Björn Trauzettel, and Fabrizio Dolcini, “Signatures of Majorana bound states in transport properties of hybrid structures based on helical liquids,” *Phys. Rev. B* **89**, 205115 (2014).
- [61] Bo Lu, Pablo Buset, Keiji Yada, and Yukio Tanaka, “Tunneling spectroscopy and josephson current of superconductor-ferromagnet hybrids on the surface of a 3d TI,” *Superconductor Science and Technology* **28**,

- 105001 (2015).
- [62] François Crépin, Pablo Burset, and Björn Trauzettel, “Odd-frequency triplet superconductivity at the helical edge of a topological insulator,” *Phys. Rev. B* **92**, 100507(R) (2015).
 - [63] Pablo Burset, Bo Lu, Grigory Tkachov, Yukio Tanaka, Ewelina M. Hankiewicz, and Björn Trauzettel, “Superconducting proximity effect in three-dimensional topological insulators in the presence of a magnetic field,” *Phys. Rev. B* **92**, 205424 (2015).
 - [64] Jorge Cayao and Annica M. Black-Schaffer, “Odd-frequency superconducting pairing and subgap density of states at the edge of a two-dimensional topological insulator without magnetism,” *Phys. Rev. B* **96**, 155426 (2017).
 - [65] Felix Keidel, Pablo Burset, and Björn Trauzettel, “Tunable hybridization of Majorana bound states at the quantum spin Hall edge,” *Phys. Rev. B* **97**, 075408 (2018).
 - [66] S. Modak, K. Sengupta, and Diptiman Sen, “Spin injection into a metal from a topological insulator,” *Phys. Rev. B* **86**, 205114 (2012).
 - [67] Abhiram Soori, Oindrila Deb, K. Sengupta, and Diptiman Sen, “Transport across a junction of topological insulators and a superconductor,” *Phys. Rev. B* **87**, 245435 (2013).
 - [68] G. E. Blonder, M. Tinkham, and T. M. Klapwijk, “Transition from metallic to tunneling regimes in superconducting microconstrictions: Excess current, charge imbalance, and supercurrent conversion,” *Phys. Rev. B* **25**, 4515–4532 (1982).
 - [69] K. Sengupta, Igor Žutić, Hyok-Jon Kwon, Victor M. Yakovenko, and S. Das Sarma, “Midgap edge states and pairing symmetry of quasi-one-dimensional organic superconductors,” *Phys. Rev. B* **63**, 144531 (2001).
 - [70] C. J. Bolech and Eugene Demler, “Observing Majorana bound states in p -wave superconductors using noise measurements in tunneling experiments,” *Phys. Rev. Lett.* **98**, 237002 (2007).
 - [71] A. R. Akhmerov, Johan Nilsson, and C. W. J. Beenakker, “Electrically detected interferometry of Majorana fermions in a topological insulator,” *Phys. Rev. Lett.* **102**, 216404 (2009).
 - [72] Yukio Tanaka, Takehito Yokoyama, and Naoto Nagaosa, “Manipulation of the Majorana fermion, Andreev reflection, and Josephson current on topological insulators,” *Phys. Rev. Lett.* **103**, 107002 (2009).
 - [73] K. T. Law, Patrick A. Lee, and T. K. Ng, “Majorana fermion induced resonant Andreev reflection,” *Phys. Rev. Lett.* **103**, 237001 (2009).
 - [74] Karsten Flensberg, “Tunneling characteristics of a chain of majorana bound states,” *Phys. Rev. B* **82**, 180516 (2010).
 - [75] Satoshi Ikegaya, Yasuhiro Asano, and Yukio Tanaka, “Anomalous proximity effect and theoretical design for its realization,” *Phys. Rev. B* **91**, 174511 (2015).
 - [76] Satoshi Ikegaya, Shu-Ichiro Suzuki, Yukio Tanaka, and Yasuhiro Asano, “Quantization of conductance minimum and index theorem,” *Phys. Rev. B* **94**, 054512 (2016).
 - [77] Bo Lu, Pablo Burset, Yasunari Tanuma, Alexander A. Golubov, Yasuhiro Asano, and Yukio Tanaka, “Influence of the impurity scattering on charge transport in unconventional superconductor junctions,” *Phys. Rev. B* **94**, 014504 (2016).
 - [78] Christoph Fleckenstein, Felix Keidel, Björn Trauzettel, and Niccolò Traverso Ziani, “The invisible Majorana bound state at the helical edge,” *The European Physical Journal Special Topics* **227**, 1377–1386 (2018).
 - [79] C. Fleckenstein, N. Traverso Ziani, and B. Trauzettel, “Conductance signatures of odd-frequency superconductivity in quantum spin Hall systems using a quantum point contact,” *Phys. Rev. B* **97**, 134523 (2018).
 - [80] Stefano Valentini, Rosario Fazio, and Fabio Taddei, “Andreev levels spectroscopy of topological three-terminal junctions,” *Phys. Rev. B* **89**, 014509 (2014).
 - [81] Pei Wang, Jie Liu, Qing-feng Sun, and X. C. Xie, “Identifying the topological superconducting phase in a multi-band quantum wire,” *Phys. Rev. B* **91**, 224512 (2015).
 - [82] Erik Eriksson, Roman-Pascal Riwar, Manuel Houzet, Julia S. Meyer, and Yuli V. Nazarov, “Topological transconductance quantization in a four-terminal Josephson junction,” *Phys. Rev. B* **95**, 075417 (2017).
 - [83] Berthold Jäck, Yonglong Xie, Jian Li, Sangjun Jeon, B. Andrei Bernevig, and Ali Yazdani, “Observation of a Majorana zero mode in a topologically protected edge channel,” *Science* **1444**, eaax1444 (2019).
 - [84] Sean Hart, Hechen Ren, Timo Wagner, Philipp Leubner, Mathias Mühlbauer, Christoph Brüne, Hartmut Buhmann, Laurens W. Molenkamp, and Amir Yacoby, “Induced superconductivity in the quantum spin Hall edge,” *Nat. Phys.* **10**, 638–643 (2014).
 - [85] Vlad S. Pribiag, Arjan J. A. Beukman, Fanming Qu, Maja C. Cassidy, Christophe Charpentier, Werner Wegscheider, and Leo P. Kouwenhoven, “Edge-mode superconductivity in a two-dimensional topological insulator,” *Nature Nanotechnology* **10**, 593–597 (2015).
 - [86] Ebrahim Sajadi, Tauno Palomaki, Zaiyao Fei, Wenjin Zhao, Philip Bement, Christian Olsen, Silvia Luescher, Xiaodong Xu, Joshua A. Folk, and David H. Cobden, “Gate-induced superconductivity in a monolayer topological insulator,” *Science* **362**, 922–925 (2018).
 - [87] Valla Fatemi, Sanfeng Wu, Yuan Cao, Landry Bretheau, Quinn D. Gibson, Kenji Watanabe, Takashi Taniguchi, Robert J. Cava, and Pablo Jarillo-Herrero, “Electrically tunable low-density superconductivity in a monolayer topological insulator,” *Science* **362**, 926–929 (2018).